Research papers

Intercomparison of recent microwave satellite soil moisture products on European ecoregions

A. Mazzariello [a], R. Albano [a,*], T. Lacava [b], S. Manfreda [c], A. Sole [a]

[a] *School of Engineering, University of Basilicata, Potenza, Italy*
[b] *Institute of Methodologies for Environmental Analysis IMAA, Italian National Research Council CNR, Tito, PZ, Italy*
[c] *Department of Civil, Architectural and Environmental Engineering, University of Naples Federico II, Napoli, Italy*

ARTICLE INFO

ABSTRACT

Several satellite microwave-based soil moisture (SM) products have become available in recent years, making possible to produce different datasets at continental and/or a global scale. Numerous variables, including geographic heterogeneity, weather and climate, and land cover, have an impact on these products' accuracy. In this study, we account for all these variables by using the ecoregions as the scale of analysis and conducting a thorough comparison of satellite products with ground-based SM measurements. The whole Europe has been selected as study area, considering it as the aggregation of several ecoregions, each of them classified as an homogeneous zones, in terms of climate, vegetation and potentially investigable soil cover. Selected SM satellite data includes: i) the National Aeronautics and Space Administration (NASA) SMAP L4 V5; ii) the European Space Agency (ESA) SMOS-IC V2.0; iii) the H115 and H116 SM products in time-series format generated by analyzing data collected by the Advanced Scatterometer (ASCAT) aboard MetOp satellites; iv) the CGLS SSM 1 km obtained by the radar onboard ESA's SENTINEL-1 platforms; and v) the European Space Agency's Climate Change Initiative for Soil Moisture (ESA CCI SM) "COMBINED" ESA CCI SM v06.1 product, created by merging satellite-based passive/active microwave measurements. Such a variety, in terms of technologies and main features, of publicly available online SM products (in their up-to-date version), allowed for a comprehensive intercomparison against in situ measurements of the International Soil Moisture Network (ISMN), that spreads across all of Europe within the above-mentioned terrestrial ecoregion, using four different metrics, i.e., r, bias, ubRMSE and r/r$_{ANOM}$.

Overall the intercomparison has underlined how SMAP L4 and ESA CCI show the best performance regardless of the considered metric. ASCAT has achieved best performances among non-modeled/blended products, while SMOS-IC has showed slightly better performance than the CGLS SSM 1 km. Using ecoregions allowed to further characterize the differences of each satellite products and identify the areas where all these products are more reliable (e.g., group (1) made by ecoregions as the Cantabrian Mixed forests or the Balkan Mixed forests; or group 2 made by ecoregions which belong to Mediterranean area) or less performing (e.g., the Central European mixed forests and the Pontic steppe). Hence, these classes have been further analyzed exploiting the ERA5-Land data, in terms of the SM, air temperature, precipitation, evaporation and Leaf area index. The research has provided helpful insights into how the performance of particular SM satellite products changes based on both the characteristics of the product under consideration and the area under investigation (i.e., one ecoregion compared to another).

1. Introduction

Soil moisture (SM) is a key element of the surface water budget, controlling numerous processes occurring at different temporal and spatial scales within the climate system (Rodríguez-Iturbe et al., 2006; Manfreda et al., 2011; Baldwin et al., 2019). It is crucial for plant transpiration and photosynthesis, impacting the water, energy, and biogeochemical cycles, as well as triggering some natural hazards (such as droughts, floods, and landslides) due to contributions to runoff and infiltration dynamics (Koster et al., 2004; Seneviratne et al., 2010; Miralles et al., 2012; Albano et al., 2017; Chen et al., 2017). Therefore, monitoring SM spatiotemporal variability has currently become one of

---

* Corresponding author.
E-mail address: raffaele.albano@unibas.it (R. Albano).

the major challenges in a rapidly changing climate. SM can be measured by direct (i.e., gravimetric technique) or indirect methods (i.e., time-domain reflectometry TDR or soil capacitance measurements) at a point scale, while large-scale information may be collected by satellite sensors or models (Seneviratne et al., 2010). Each approach has its own pros and cons, and their integration usually provides the best performance in retrieving SM information (Lacava et al., 2013).

Focusing on remote sensing, the capability of satellite sensors to acquire data useful for SM retrieval and investigation has been largely demonstrated in recent years (Ochsner et al., 2013), especially using measurements collected in the microwave region of the electromagnetic spectrum (Kerr, 2007; Wagner et al., 2007; Scarpino et al., 2018). Both passive (i.e., radiometer) and active (i.e., radar or scatterometer) sensors can, in fact, provide useful information about SM in the surface soil layer (up to 5–10 cm; hereafter referred indifferently to as SSM or SM) with different spatial and temporal resolutions depending on the features of the platform/sensor system used (Gao et al., 2006; Escorihuela et al., 2010; Manfreda et al., 2014). Two satellite missions created specifically for SM recovery were launched and are currently in operation because of the SM's usefulness in the spectrum of scientific applications referred above. The first one was the Soil Moisture and Ocean Salinity (SMOS) mission (Kerr et al., 2010), launched in 2009, followed in 2015 by the Soil Moisture Active and Passive (SMAP) mission (Entekhabi et al., 2010a). Both these missions, notwithstanding failure of the active system of SMAP soon after its launch, can provide SM measurements with a sub-weekly temporal resolution and a spatial resolution of a few kilometers. Other satellite sensors have demonstrated their potential for SM retrieval at similar resolutions, such as the Advanced Scatterometer (ASCAT) onboard MetOP satellites (Wagner et al., 2013), as well as the recent radar onboard the Copernicus Sentinel-1 mission (Bauer-Marschallinger et al., 2019). The Advanced Microwave Scanning Radiometer 2 (AMSR-E2) onboard the Global Change Observation Mission (GCOM-1) is another instrument used for SM evaluation owing also to the experience developed on AMSR-E, its forerunner on Aqua satellite (Lacava et al., 2013). Furthermore, data from a few of the above-mentioned sensors/missions have been blended in the framework of the ESA Climate Change Initiative (CCI) program, to provide the so-called ESA CCI global satellite-observed SM dataset (Dorigo et al., 2017; Gruber et al., 2019). A large number of calibration/validation experiments have been carried out so far to assess the accuracy of several SM products (Wigneron et al., 2007; Rodríguez-Fernández et al., 2017; Chen et al., 2017), whose quality have quickly improved in the meanwhile due to the development of new approaches, parameterizations, and concepts.

Apart from a large series of works focused on the comparison between remote and in situ SM measurements at the single scale of the satellite pixel encompassing the ground station/s (Lacava et al., 2012), others have been conducted at a regional and/or global scales (Brocca et al., 2011; Ray et al., 2017), extending at the selected larger spatial scale achievements related to the ground-based measurements, regardless of their often heterogeneous spatial distributions. Among the works that focus on narrow specific areas such as in Spain, Italy, France or USA (Brocca et al., 2011; Cui et al., 2017; El Hajj et al., 2018), many of them present comparisons of different SM datasets with in-situ data, showing not homogeneous results, depending on the data considered, as well as on the specific site-condition of the area analyzed. For example, ASCAT performed better than AMSR-E in Spain, Italy, and France (Brocca et al., 2011), SMAP was found better than the other sensors in Spain and USA by Cui et al. (2017), while the work by El Hajj et al. (2018) highlighted the relevant impact of Radio Frequency Interference (RFI) on SMOS product performances.

Other studies at continental/global scale (Colliander et al., 2017; Liu et al., 2019; Min et al., 2022) tried also to include in the analysis factors, such as climate and/or vegetation characteristics, that might change on the basis of the considered scale of investigation and cause the above-mentioned discrepancies among different regions (e.g., Al-Yaari et al.,

2014). In particular, Al-Yaari et al. (2019) conducted a global study at three levels considering: the five continents first, the Koppen-Geiger climatic zones (Rubel et al., 2017) and finally at the vegetation scale, referring to International Geosphere-Biosphere Programme (IGBP) land cover classification (Friedl et al., 2010). The study evidenced that satellites have variable performance in Europe, which deserves further investigation. However, Min et al. (2022) provided evidence that Radio Frequency Interference (RFI) is a problem that might have a considerable impact on the comparison in Europe.

It is important to note that although soil and climate can be thought of as external factors, soil moisture dynamics depends on the reciprocal relationships between vegetation and water availability (Porporato and Rodriguez-Iturbe, 2002). As a result, the analysis that was done by taking variables like vegetation or climate into account separately did not allow for a thorough evaluation of SM performances. On the contrary, taking into account the combination of climate and vegetation could allow to better understand which one or which combination of factors introduces errors in the microwave SM products, as well as justifying why Europe (EU) had poor (in some cases) and a diversity of performance in previous studies.

In addition, the choice of the reference scale is also a critical issue which may impact on the performance assessment. For instance, the field scale appears too specific to guide on the choice of a satellite product, while global intercomparisons generalize the problem too much, making comparison not always easy.

By contrast, the current study, starting from the results of Al-Yaari et al. (2019), explores the behavior of SSM products in the EU grouped by ecoregions to implement an intercomparison assessment in areas defined according to the combination of different flora, fauna, and climatic characteristics. Indeed, the study aims to expand the understanding of a mid-scale analysis to evaluate the various roles played by the combination of elements in SM satellite retrievals in Europe. Effectively, ecoregions are defined as relatively large land areas characterized by a peculiar assemblage of natural communities and species, with boundaries that approximate the original extent of natural communities prior to major land-use change (Olson et al., 2001). The use of ecoregions for SM assessment, here for the first time applied in Europe, has been already tested in USA by Baldwin et al.(2017), demonstrating its feasibility, because the variability of SM with respect to the ground measurements within each ecoregion was found lower that the one from neighboring ecoregions.

The SM satellite products, analyzed in this study, are the NASA SMAP Level 4 V5 (SMAP L4), ESA SMOS-IC, ASCAT (H115 & H116), the CGLS SSM 1 km and the CCI long-term record SM (V04.2). Each of them was selected as the most up-to-date version of the products at the time of investigation and representative of different technologies (i.e., active or passive sensors) and approaches (i.e., modelled and/or blended) at different spatiotemporal resolution. Evaluation of the products was carried out through in situ SM measurements from the International Soil Moisture Network (ISMN) observed at a depth of 5 cm, generally assumed as satellite microwave sensing depth (Qiu et al., 2016), in the period from January 2015 to December 2020. Two years of measurements were at least available for all the considered SM products in such a 5-year temporal interval.

The paper is organized in the following way: the European ecoregions investigated and their features as well as the satellites and ground-based datasets or methods and scores used for satellite product evaluation are described in Section 2. Results are presented in Section 3 and Discussions are shown in Section 4. Finally, Section 5 summarizes the main Conclusions.

2. Material and methods

2.1. The European ecoregions

In 1996, the WorldWide Fund (WWF) for Nature launched the

"Global 200 Initiative," a campaign to promote biodiversity conservation (Bulgarini et al., 2004), and making a digital map of 867 terrestrial ecoregions (https://ecoregions.appspot.com/). These ecoregions should be a priority for implementing conservation actions in relation to their outstanding biodiversity features in the terrestrial, freshwater, and marine realm (Olson et al., 2001; Olson and Dinerstein, 2002). Their boundaries have been determined using a combination of existing global maps, such as zoogeographic (Rübel, 1930), biotic provinces (Dasmann, 1973, 1974), and vegetation types (UNESCO, 1969).

Dinerstein et al. (2017) improved the delimitation in the original Terrestrial Ecoregions (Olson and Dinerstein, 1998; Ricketts et al., 1999) to better highlight regions of the world that are highly distinctive and deserve greater attention for their peculiar habitats.

Europe belongs to the Palearctic biogeographic realm and contains six biomes (i.e., boreal forests/taiga; Mediterranean forests, woodlands & scrub; temperate broadleaf & mixed forests; temperate conifer forests; temperate grasslands, savannas & shrublands; tundra) and 37 terrestrial ecoregions ranging from Mediterranean-climate woodlands and scrub to temperate rainforests or tundra. All together, these ecoregions span an area larger than the European territory, including a subset of north-west Asia. Hence, in this study, we refer to these areas as "continental" or "European" scale. Ecoregions are not equally represented both by the number of ISMN monitoring stations and by their spatial distribution over the area. Fig. 1 represents the ISMN ground-stations, aggregated using different symbols by local network managed by different individual organizations/institutes, above the ecoregions considered in this study identified by a unique code and color. For a detailed description of the ISMN network used, please see Section 2.1.1.

It is evident that there are a few ecoregions represented by ground-based stations concentrated only in a defined sub-sector. According to the SM temporal stability concept (Vachaud et al., 1985; Cosh et al., 2006; Starks et al., 2006; Brocca et al., 2009; Liu et al., 2011; Loew and Schlenz, 2011; Brocca et al., 2011), local SM signal can be representative of larger areas, considering that the temporal pattern of point SM data is closely related to the temporal pattern of its surrounding area (Brocca et al., 2011). This implies that persistent regional SM patterns can influence individual zones within a region, resulting in similar SM dynamics. Therefore, it is acceptable to use datasets that describe SM in the same way but are recorded at different scales. In line with this approach, we aggregated results from non-homogeneously or sparsely distributed ground stations (in terms of median values) to represent the entire ecoregion, following the methodology used by Baldwin et al. (2017) in the USA. Furthermore, it is worth noting that, as we said above, ISMN stations are randomly spatially distributed in Europe, with some of the EU ecoregions completely uncovered. Therefore, it was possible to make the comparison of SM satellite products and ground measurements only in 16 of the 37 above-cited ecoregions. The main features of the considered ecoregions, including their specific Koppen-Geiger climate classification, are described in Table A.1 of the Appendix A of supplementary data.
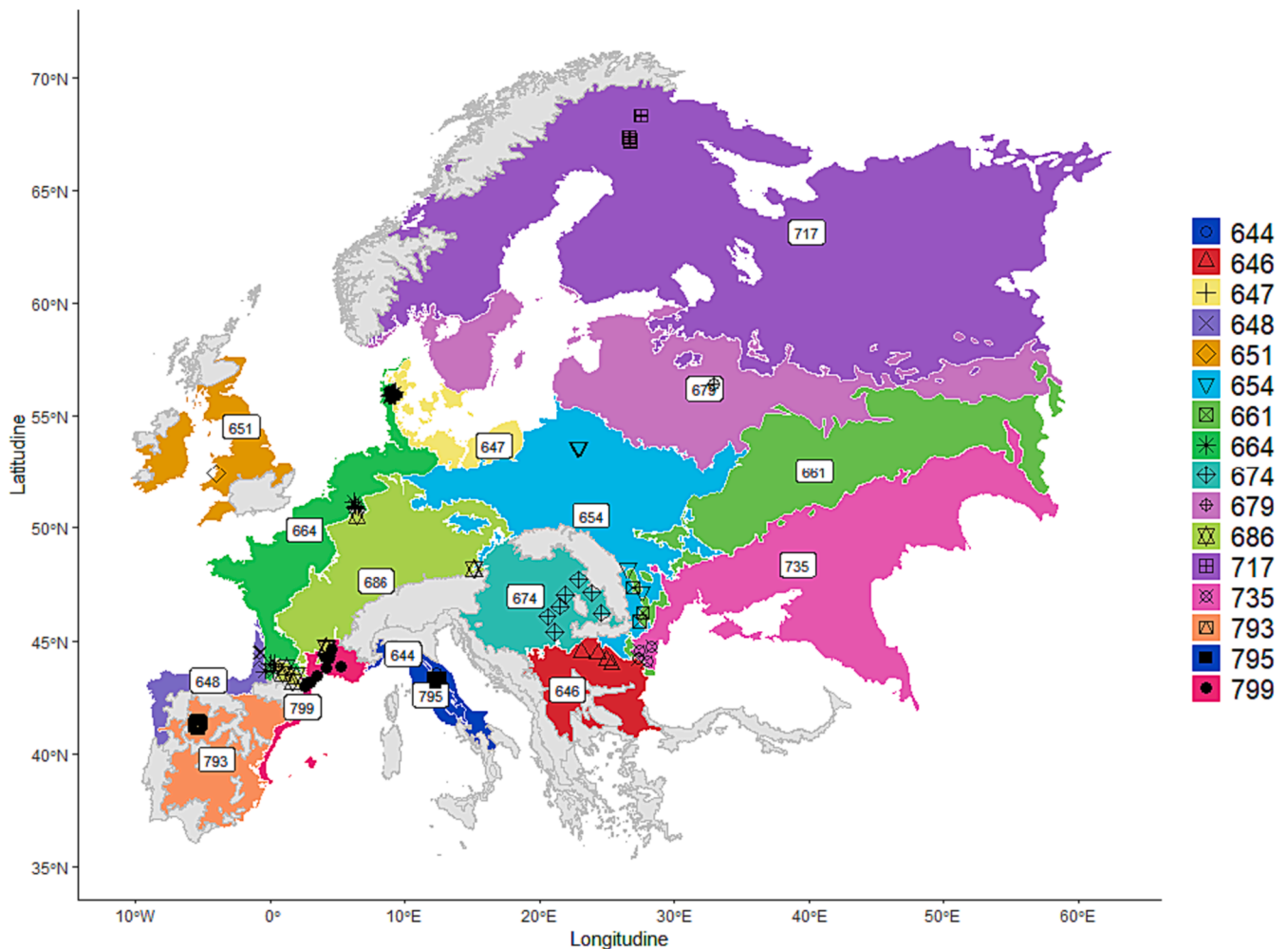

Fig. 1. Distribution of the 16 ecoregions considered in this study, spanning an area larger than the European territory, including a subset of north-west Asia and location of the used ISMN stations indicated using different symbols for each local network.

2.2. Dataset description

The SM data used in this study were obtained from the International Soil Moisture Network (ISMN) and from ESA (SMOS, METOP A & METOP B, Copernicus Sentinel 1, ESA CCI) and NASA (SMAP) satellite missions/platform. In the following their main features will be briefly described.

2.2.1. The International soil moisture network

Since 2009, the ISMN has helped with calibration and validation efforts of SM retrievals (Dorigo et al., 2011, 2013), gathering and harmonizing data from diverse organizations and improving the integration of advanced quality control methods (Dorigo et al., 2013), provision of additional metadata, and ancillary variables (e.g., precipitation, soil and air temperature). The ISMN data are available at data host facility of TU Wien under supervision of the BfG Federal Institute of Hydrology (https://ismn.geo.tuwien.ac.at/). Currently, the European ISMN network is composed of 28 station networks that are not evenly distributed and some of which are not operational (Dorigo et al., 2021). SM data are provided at several depths depending on the site in terms of volumetric water content (VWC m^3/m^3) and are accompanied by quality flag indicators.

In our study, we chose only the ISMN stations within the selected ecoregions having SM measurements at a depth of 5 cm from January 2015 to December 2020. In addition, only measurements flagged as "good" and with the VWC between 0–0.6 m^3/m^3 were considered (Dorigo et al., 2013; Al-Yaari et al., 2019). Among the existing networks, nearly 200 ground stations are available representing the 16 ecoregions reported above (Fig. 1). Table 1 summarizes some features (Dorigo et al., 2021) of the chosen networks (name, location, number of gauge stations and activity status).

The ISMN is given by the combination of several networks which are managed by individual institutes or agencies. This leads to a heterogeneous distribution of the monitoring stations which are clustered in specific locations. In the following more details are included for each ecoregion and relative ground stations local network(s) that fall within:

- The Italian sclerophyllous and semi-deciduous forests (795) share the Umbria network with the Appenine deciduous montane forests (644), which also contain the HYDROL-NET_PERUGIA. In both cases stations are located in the Central part of Italy.
- The Romanian monitoring network, RSMN, covers five ecoregions: the Balkan Mixed forests (646), the Pannonian mixed forests (674), the Pontic steppe (735), the East European forest steppe (661), and the Central European mixed forests (654). The ground-based monitoring stations are located respectively on the border with Bulgaria; between Romania and Hungary; in the Black Sea region of Romania and finally on the border with Moldova for both the 661 and 654

ecoregions. In addition, the Central European mixed forests (654) host the BIEBRZA_S-1 network, located in northern Poland.
- The Celtic broadleaf forests (651) is described by the WSMN network which is located in the United Kingdom.
- The European Atlantic mixed forests (664) overlap with the Baltic mixed forests (647) in the Hobe monitoring network and with the Northeast Spain and Southern France Mediterranean forests (799), Western European broadleaf forests (686), and Cantabrian mixed forests (648) in the SMOSMANIA network. Furthermore, the European Atlantic mixed forests and Western European broadleaf forests (686), which encompasses the HOAL monitoring network, also share the TERENO network. The SMOSMANIA network extends to the Mediterranean coasts (799) and covers the Occitania (664) and Aquitaine (686 and 648) regions, while the HOBE network is centered in Denmark and the HOAL network is centered in Austria. The Aquitaine region has additional monitoring capabilities through the Fr_Aqui network, which is integrated into the Cantabrian mixed forests (648).
- The Sarmatic mixed forests (679) encompass the Ru_CFR network which belong to Russian area.
- The Scandinavian and Russian taiga (717) include the FMI network which covers a northern part of Finland.
- The Iberian sclerophyllous and semi-deciduous forests (793) is monitored by the REMEDHUS network, mostly located in the northern part of Spain.

2.2.2. The SM satellites products

The diverse satellite SM datasets selected for this study are listed in Table 2 that provides their main technical features.

2.2.2.1. SMOS – IC.
The SMOS mission was launched in November 2009 by the European Space Agency as the first explorative mission able to provide observations of SM and sea surface salinity exploiting the exchange in the Earth's water cycle between land and the atmosphere using MIRAS microwave L-band (1.4 GHz) measurements. Among the globally available products, we used the SMOS-IC v.02 at 25 km of spatial resolution, available in both ascending (i.e., 06:00 a.m.) and descending (i.e., 06:00p.m.) orbits. The SMOS-IC minimizes the use of auxiliary data (e.g., the Moderate Resolution Imaging Spectroradiometer (MODIS), Leaf Area Index (LAI)), exploiting the ISMN in situ observations and global maps of Parrens et al. (2016) to optimize the effective vegetation scattering albedo (ω) (Fernandez-Moran et al., 2017) and the roughness parameters, respectively.

We have filtered out the signals affected by potential RFI contamination by masking out the ones when root mean square error between SMOS L3 and simulated Brightness Temperature (TB-RMSE) were higher than 10 K (Al-Yaari et al., 2019; Wigneron et al., 2020) and the strong topography, frozen scene, and contaminated scene (urban + ice + water bodies) by masking out scene flags (SF) <=1 (Li et al., 2020; Wigneron et al., 2021; Li et al., 2021).

2.2.2.2. SMAP L4.
In 2015 the NASA SMAP satellite mission was launched to provide information on surface soil moisture, on the freeze/thaw state of the land surface, on root zone SM until 1 m (Reichle et al., 2014; Derksen et al., 2017), and net ecosystem exchange (NEE) of carbon. The SMAP satellite is equipped with a radiometer working in L-Band at a spatial resolution ~36 km and a radar that functioned only for a few months in 2015 at a frequency of 1.26 GHz and a spatial resolution ~3 km. Among the different available half-orbit SM products (e.g., SMAP L2, SMAP L3), we used the model assimilated product SMAP L4 v6 (Data Set ID: SPL4SMAU) at 3-h time resolution on the global 9 km modeling grid.

The SMAP L4 assimilates the 36 km brightness temperature (from L1C_TB), the 9 km brightness temperature downscaled by the L2_SM_AP algorithm and freeze/thaw observations (from L3_FT_A) using an

Table 1
Local networks included in the ISMN that have been adopted in the present study.

Name	Location	n. stations	Status
WSMN	UK	8	Running
UMBRIA	Italy	13	Running
TERENO	Germany	5	Running
SMOSMANIA	France	22	Running
Ru_CFR	Russia	2	Running
RSMN	Romania	20	Running
REMEDHUS	Spain	24	Running
HYDROL-NET_PERUGIA	Italy	2	Running
HOBE	Denmark	32	Inactive
HOAL	Austria	33	Running
FR_Aqui	France	5	Running
FMI	Finland	27	Running
BIEBRZA_S-1	Poland	30	Running

Table 2
SM satellite retrieval technical features.

Mission/Platform	Sensor	Type	Version	Temporal Resolution (Acquisition time, when available)	Time period[1]	Spatial coverage	Spatial sampling
SMOS	MIRAS	Passive	SMOS-IC	12 h (6:00 a.m. 6:00p.m.)	2010-present	Global	25 km
SMAP	SAR & RADIOMETER	Passive	SMAP L4 V5	3 h-	2015-present	Global	9 km
METOP A & METOP B	ASCAT	Active	H115 & H116	12 h (9:30 a.m. 9:30p.m.)	2007-present	Global	12.5 km
Copernicus Sentinel 1	SAR	Active	SSM − 1 km V1	1.5–4 days	2015-present	Europe	1 km
ESA CCI		Combined	ESA CCI v06.1	Daily	1978–2020	Global	0.25°

[1] A common timeframe (2015–2020) was chosen in this study.

ensemble Kalman filter (EnKF, Reichle et al., 2014). No filter was applied on the product.

2.2.2.3. ASCAT. One of the instruments carried on board ESA's MetOp satellites (MetOp -A launched in 2006, MetOp -B launched in 2012 and MetOp -C launched in 2018) is the Advanced Scatterometer (ASCAT). Such a sensor operates in the C-band (5.3 GHz) with vertical polarization (VV). The MetOp satellites are ~50 min apart from each other with 09:30 a.m. descending and 09:30p.m. ascending orbits, respectively. Using a change detection method developed at the Institute of Photogrammetry and Remote Sensing (IPF), of the Vienna University of Technology (TU Wien), SSM data in degree of saturation (Wagner et al., 1999) are retrieved from the backscattering measurements.

The study was conducted with the Metop ASCAT surface SM climate data records (CDRs), specifically, the H115 – Metop ASCAT SSM CDR2019 and its temporal extension H116, at a spatial resolution of 12.5 km, expressed in terms of degrees of saturation, converted to physical units in meters using a globally and high-resolution porosity map with average polygon size ~100 km (Gleeson et al., 2014). During our analysis, SSM was excluded when its value was lower than 0 or greater than 100, or the processing flags (PROC_FLAG) indicated that no retrieval was carried out (e.g., PROC_FLAG > 1) or the surface state flag (SSF) indicated the following soil surface conditions: unknown, unfrozen, frozen, temporary melting/water on the surface or permanent ice.

2.2.2.4. SSM CGLS 1 km. The Copernicus Global Land Service (CGLS) has "a multi-purpose service component" providing a series of biogeophysical products on the status and evolution of land surface at global scale, such as the SSM CGLS 1 km, namely surface soil moisture (in terms of saturation degree) at 1 km (1°/112) spatial sampling. The SSM CGLS 1 km is derived from microwave radar data observed by the Sentinel-1 SAR satellite sensors (C-band) with a temporal resolution over Europe of 1.5–4 days starting from 2016 (the temporal resolution was about 3–8 days before 2016), when both Sentinel 1A and B became available.

The Sentinel-1 backscatter value, terrain-geo-corrected and radiometrically calibrated, is used to obtain soil moisture applying an adaption of the TU-Wien-Change-Detection (Wagner, 1998). The algorithm modified by Pathe et al. (2009), has been used both for low resolution ERS and ASCAT data and for higher resolution SAR validating it over Australia, Africa and large parts of South America (Algorithm Theoretical Basis Document CGLS SSM 1 km, Bauer-Marschallinger et al., 2019).

A few filters were already considered within the algorithm hence, no further analysis was carried out. As for ASCAT, to compare SSM CGLS 1 km with ground-based measurements, the Gleeson's globally-high resolution porosity map is used (Gleeson et al., 2014) with the aim to move to volumetric soil moisture content.

2.2.2.5. ESA CCI. The combined ESA CCI-SM product blends scatterometer-based (ERS- ½, Metop A/B ASCAT) and radiometer-based SM information (SMMR, SSM/I, TMI, AMSR-E, WindSat, AMSR-E2, and SMOS), utilizing a weighted normal technique with the loads being relative to signal to noise ratio (SNR) assessed by the triple collocation investigation of every item (Dorigo et al., 2017; Gruber et al., 2019). A CDF matching procedure is used before integrating all datasets to scale the SM into the Noah land surface model by the Global Land Data Assimilation System (GLDAS) (Rodell et al., 2004).

The day-by-day information provided concerns VWC (m^3/m^3) at a spatial resolution of 0.25° × 0.25°, distributed in NETCDF format. We refer to the ESA CCI v6 product, ending in 2020.

Data related to pixel locations covered by snow or with temperatures below 0 °C or covered by dense vegetation have been filtered out.

2.3. Methods

Our analysis compares satellite SM products with ground-based data from the ISMN, using all available observations in the 2015–2020 period (in instantaneous overpass times), when all data were available to avoid gaps.

Furthermore, we evaluated our results by using SM time series extracted from the original grids (e.g., 9 km for SMAP L4, 25 km for SMOS-IC) for those pixels that correspond to each station separately (based on its latitude and longitude). It is possible that some stations in a dense network correspond to the same passive (SMAP, and SMOS), blended (CCI) pixel and several active (ASCAT) pixels. SM satellite retrievals were matched with instantaneous in situ measurements within a time window of 1 h and the pairs are aggregated in a "daily" time step. The metrics between satellite data and the in-situ observations were then computed separately for each station. Finally, the median of each metric for all stations within an ecoregion was calculated.

It is notable to mention that the different re-mapping grids of satellite data (e.g., WARP, SMOS, Quarter-Degree-Grid) as well as the scale discrepancies between in situ and satellite data, might have impacted the uncertainty of our results, in addition to the aggregation at ecoregion scale (as the largest homogeneous area potentially investigated) accordingly with the concept of temporal stability already discussed in Section 2.1. However, this issue is out of the scope of the present work and, therefore, it isn't further investigated here.

Three main scores, widely used within the SM community (Entekhabi et al., 2010b; Al-Yaari et al., 2019; Peng et al., 2021; Zheng et al., 2022), were considered to evaluate remotely sensed SM products accuracy: Pearson correlation coefficient (r), bias, and unbiased root mean square error (ubRMSE). r is unconcerned with any bias in the mean or magnitude of the variations; while the ubRMSE is a measure of accuracy after removing of sensitivity to distortions in both mean and amplitude of fluctuations, exploiting bias. This latter metric incorporates the RSME, which removes only the amplitude of fluctuation (Entekhabi

et al., 2010). Please, see Al-Yaari et al., 2019; Peng et al., 2021; Zheng et al., 2022 for the formulation.

The performance of the analysis carried out considering an historical series may be positively affected by the seasonal cycle (Scipal et al., 2008). Therefore, we have also considered to evaluate SM anomalies, computed, for example, as proposed by **Rodríguez-Fernández et al. (2016) on the basis of a 35-day moving window (w) (Brocca et al., 2011) in order to better assess the accuracy of the SM products.

$$SM(t)_{ANOM} = \frac{SM(t) - \overline{SM(t-17:t+17)}}{sigma_{SM}(t-17:t+17)} \qquad (1)$$

where the anomalies ($SM(t)_{ANOM}$) could be generically referred to the satellite (SAT) or the in situ (ISMN) SM time-series, and computed as deviation of a measured acquired at time (t) from the SM mean $\overline{SM(t)}$ evaluated on a temporal interval ranging from previous 17 day before (t) and next 17 days after (t). Such a deviation is weighted by the SM standard deviation ($sigma_{SM}$) computed on the same period. Such a formulation allows for a rough reduction of seasonality effects, and hence to analyze short-term variations. To completely remove the seasonality, we should consider a long-term analysis that will be proposed in a companion study.

SM anomalies are first exploited to detect outliers, finding, and discarding the outer fences of the satellite SM anomalies dataset with the quartiles method (Walfish, 2006). Then, consistently with previous SM assessment, the metric such as the Pearson correlation coefficient (r_{ANOM}) are evaluated on a single station and then aggregated at the ecoregions scale using as a reference value the median.

3. Results

Considering that past studies highlighted that European heterogeneity in climate and habitat affected remotely sensed SM products accuracy, the results obtained in the present study can show how the combination of these factors affects satellite products' performance when considering every single European ecoregion as a homogeneous area.

In detail, the performances of each satellite SM product with respect to in situ measurements are shown in Fig. 2 in terms of median values of r, bias and ubRMSE using as refence period 2015–2020.

The overall analysis demonstrated that the performances of each satellite product are strongly influenced by ecoregions' spatial heterogeneity, climatic conditions and land cover. All satellite products show weak performances for all metrics on i) the Pontic steppe ecoregion (735) and ii) the Central European mixed forest (654). It is worth mentioning that the ecoregions 735 and 654 are contiguous.

In the following, we present the results of intercomparison between different remote sensing products detailed for each metric. In terms of r, SMAP L4 showed the best performance in the most part (i.e., eleven) of ecoregions, ESA CCI in four and ASCAT performed better than the other satellite products on the Pontic steppe ecoregion (735), providing a correlation value of 0.36. On the other hand, CGLS SSM 1 km showed the lowest correlations with ground data in the most part (i.e., ten) of ecoregions, SMOS-IC on five ecoregions and ESA CCI on the ecoregion 654 (where, as we said above, all SM products have weak performances). In particular, CGLS SSM 1 km did not show any correlation in Sarmatic mixed forests (679) and Scandinavian and Russian taiga (717) ecoregions, obtaining an r close to 0. The SMOS-IC had variable correlations, with a value greater than 0.5 only on four of the 16 ecoregions considered in this study. Moreover, it is necessary to clarify that ESA CCI did not provide SM measurements for the considered period on the Celtic broadleaf forests ecoregion (651), where generally all SM satellite retrievals had unsatisfactory correlation except SMAP L4 (r = 0.62); and that we obtained meaningful correlation (r > 0.5) for all satellite products in the Balkan (646) and Baltic (647) mixed forests.

SMAP L4 exhibited the lowest values of bias (in absolute terms ranging 0.03–0.05) on eight ecoregions, except for Balkan mixed forests (646), East European Forest steppe (661), Pannonian mixed forests (674), and Pontic steppe (735) where its performance fairly decreases until reach the worst performance in 735 respects to all other satellite products. However, SMAP L4 confirmed its good performance also on Celtic broadleaf forests (651), i.e., the bias value was around 0.03, where other remote sensing products showed higher bias values. On three ecoregions (i.e., 646, 686 and 795) ESA CCI showed a
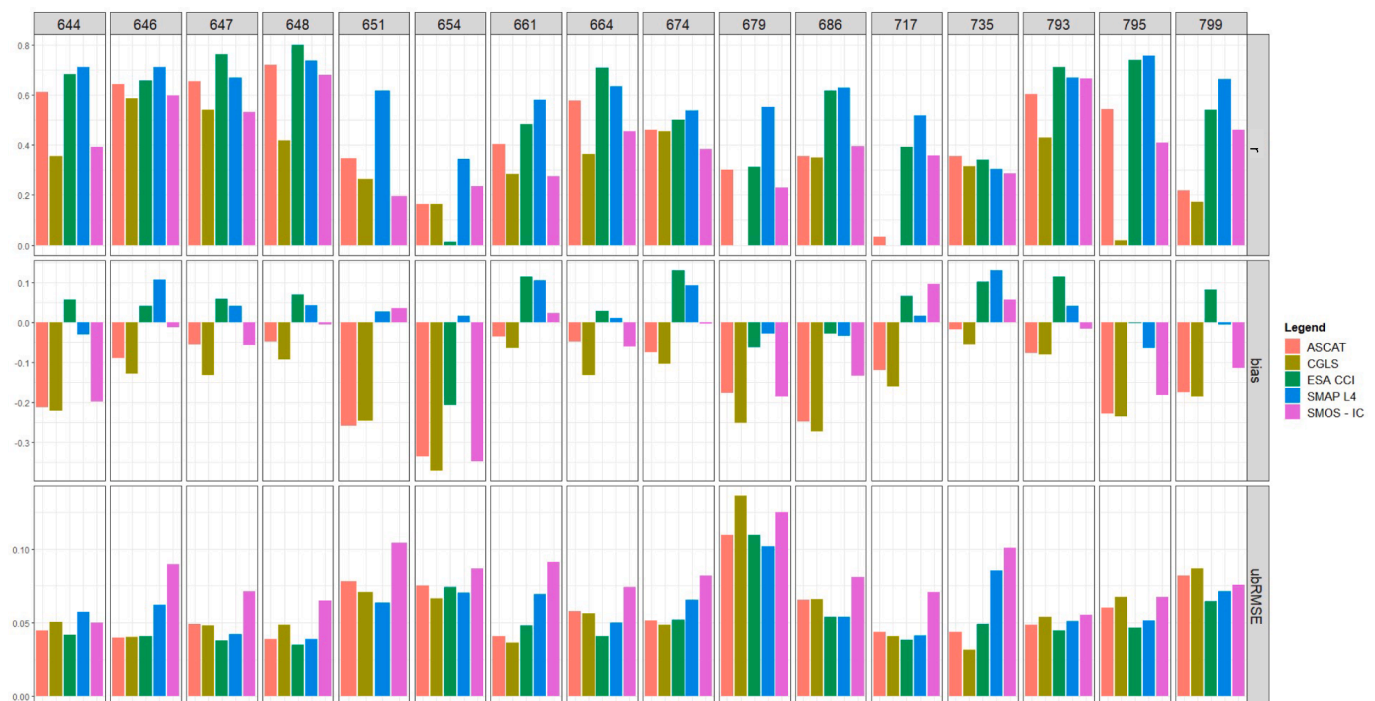

Fig. 2. Satellite products performances for each ecoregion: top panel r, middle bias and low ubRMSE.

complementary behavior to SMAP L4, obtaining the lowest value of bias. ASCAT achieved an overestimation on all ecoregions and had a better bias (i.e., close to 0) than the others on the Pontic steppe ecoregion (735) but it obtained the worst bias (−0.26) in Celtic broadleaf forests (651). SMOS-IC achieved the best performance in terms of bias only in four ecoregions (648, 661, 674, 793), while CGLS SSM 1 km had the worst values in most part of ecoregions, with a maximum value of – 0.37 on Central European mixed forest (654). More in general, a negative bias for all products was found for Sarmatic mixed forests (679) and Western European broadleaf forests (686). Instead, all remotely sensed products have a bias close to 0 in Cantabrian mixed forests (648).

In terms of ubRMSE, ESA CCI showed the best performance in most part of ecoregions as reported in Table 4; the SMAP L4 maintained a ubRMSE always comparable to ESA CCI, achieving the lowest ubRMSE in the 651 and 679 ecoregions. SMOS-IC achieved the worst bias in the most part (eleven on 16) of the ecoregions, while ASCAT and the CGLS had variable performances according to the ecoregions.

Furthermore, we also evaluated the correlation between SM anomalies (r_{ANOM}) computed using a moving window of 35 days, both calculated on situ and satellite data, to assess whether seasonality could have affected results in the different ecoregions. SMAP L4 achieved a meaningful correlation on anomalies ($r_{ANOM} > 0.5$) in five ecoregions (644, 646, 648, 654, 674). ESA CCI had a positive correlation on three of ecoregions (647,648,795), ASCAT on one (664), and the others had non-meaningful correlation. The SMOS-IC and the CGLS SSM 1 km had a nonpositive correlation.

Focusing specifically on comparing r and r_{ANOM} (hereafter referred to as r/r_{ANOM}), Table 3 displays r_{ANOM} for each sensor in each ecoregion, in comparison with those achieved on the original time-series data (r). It's worth noting that the r values in Table 3 may differ slightly from those in Fig. 2, as they were recalculated after removing outliers with the quartiles' method (as described in methodology section). Previous studies (Scipal et al., 2008; Brocca et al., 2011) have shown that, when

high seasonality is present, r tends to be greater than r_{ANOM}. As expected, removing the seasonal effect typically resulted in a decrease in correlation, with r_{ANOM} being lower than r (as shown in the white rows of Table 3). On the other hand, an increase in the correlation between r_{ANOM} and r is indicative of high signal variability or poor sensor quality in detecting SM-related signals (as shown in the dark gray rows of Table 3), considering the adopted screening out of anomaly-outliers. In Table 3 we have also reported the values of r and r_{ANOM} for each satellite aggregated at the EU continental scale, aggregating correlations by median. Examining this median value of the r and r_{ANOM} by satellite, the effect due to the procedure of screening out anomaly-outliers, was lost on the aggregation at European scale (see last line of Table 3). It confirms that the ecoregion scale is optimal for obtaining valuable information about the performance of satellites that would otherwise be lost. Probably, this is due both to the scale, neither too large nor too small but also to the combination of the factors from which the ecoregion originates (e.g., climate or vegetation).

4. Discussion

Satellite-based SM measurements accuracy may be affected by several levels of uncertainty depending on the characteristic of the considered product, as well as of the investigated area. In this work, we tried to better assess this aspect by comparing different SM products with ground measurements in the European ecoregions considered as areas with homogenous patterns related to climate, vegetation, soil cover and their interactions.

Table 4 shows the remote sensing product that obtains best performance when comparing with in-situ measurements for each ecoregion using the different metric investigated. The overall results (please see last column) show a slightly higher performance of SMAP L4 and ESA CCI, probably due respectively to the use of ancillary data such as meteorological forcing and parameterization schemes (Tavakol et al.,

Table 3
Performance obtained on each ecoregion in terms of r and r_{ANOM}. The increasing in the correlation between r_{ANOM} and r is colored in dark gray.

	ASCAT		CGLS		ESA CCI		SMAP L4		SMOS-IC	
Ecoregions	r	r_{ANOM}	r	r_{ANOM}	r	r_{ANOM}	r	r_{ANOM}	r	r_{ANOM}
644	0.6121	0.3629	0.3576	0.2112	0.6788	0.4204	0.71	0.5177	0.3905	0.3209
646	0.642	0.4058	0.5762	0.4163	0.6577	0.4842	0.7111	0.5466	0.5868	0.3496
647	0.6532	0.4435	0.5443	0.2468	0.7602	0.5467	0.6685	0.4547	0.5293	0.3165
648	0.721	0.5907	0.4663	0.424	0.7991	0.6105	0.7364	0.5866	0.6957	0.5079
651	0.2919	0.3228	0.037	0.3589	No data available	No data available	0.6224	0.4311	0.1536	0.1993
654	0.1892	0.3586	0.1636	0.2695	0.0446	0.313	0.343	0.5462	0.1771	0.4713
661	0.3988	0.4834	0.2801	0.4592	0.4806	0.4814	0.5797	0.4899	0.2726	0.3763
664	0.5773	0.4121	0.3565	0.3085	0.7132	0.4781	0.6341	0.4359	0.4626	0.2466
674	0.4576	0.4156	0.4564	0.3988	0.4903	0.4477	0.5394	0.5056	0.379	0.3113
679	0.2946	0.1712	0	0.3657	0.3125	0.2821	0.5514	0.3718	0.2362	0.1796
686	0.351	0.2202	0.3417	0.113	0.6107	0.357	0.6262	0.3772	0.3876	0.2175
717	0.0409	0.0859	0	0.0915	0.4043	0.3705	0.5845	0.4175	0.3162	0.3473
735	0.3551	0.2198	0.3422	0.1061	0.3467	0.4258	0.3129	0.3863	0.2611	0.3797
793	0.6014	0.364	0.4513	0.2298	0.7083	0.4576	0.6681	0.4458	0.6669	0.3662
795	0.5443	0.479	0.0353	0.3431	0.7331	0.5038	0.7551	0.4286	0.4166	0.3876
799	0.2233	0.1167	0.1582	0.1598	0.5365	0.2344	0.6618	0.3385	0.46	0.2359
Median at EU scale	0.4282	0.36345	0.34195	0.289	0.6107	0.4477	0.63015	0.44085	0.38905	0.3341

Table 4

Summary results of all performance (R, bias, ubRMSE, comparison between R and R_{ANOM}). Each color indicates a satellite product: light blue SMAP L4; green ESA CCI; purple SMOS-IC; orange ASCAT; and dark yellow CGLS.

Ecoregions	r	bias	ubRMSE	r/r$_{ANOM}$	Overall
644	SMAP L4	SMAP L4	ESA CCI	SMAP L4	SMAP L4
646	SMAP L4	SMOS-IC	~~ASCAT ESA CCI~~	SMAP L4	SMAP L4
647	ESA CCI	SMAP L4	ESA CCI	ESACCI	ESACCI
648	ESA CCI	SMOS-IC	ESA CCI	ESACCI	ESACCI
651	SMAP L4	SMAP L4	SMAP L4	SMAP L4	SMAP L4
654	SMAP L4	SMAP L4	CGLS	-	-
661	SMAP L4	SMOS-IC	CGLS	SMAP L4	SMAP L4
664	ESA CCI	SMAP L4	ESA CCI	ESACCI	ESA CCI
674	SMAP L4	SMOS-IC	CGLS	SMAP L4	SMAP L4
679	SMAP L4	SMAP L4	SMAP L4	SMAP L4	SMAP L4
686	SMAP L4	ESA CCI	~~SMAP L4 ESA CCI~~	SMAP L4	SMAP L4
717	SMAP L4	SMAP L4	ESA CCI	SMAP L4	SMAP L4
735	ASCAT	ASCAT	CGLS	-	-
793	ESA CCI	SMOS-IC	ESA CCI	ESACCI	ESA CCI
795	SMAP L4	ESA CCI	ESA CCI	ESACCI	ESA CCI
799	SMAP L4	SMAP L4	ESA CCI	SMAP L4	SMAP L4

2019) within advanced models or due to the combination of different satellite data. The overall lowest performance of SMOS-IC and of the high spatial resolution product CGLS SSM (1 km) could be influenced by the strong RFI in Europe (Oliva et al., 2012; Mohammed et al., 2016) as reported in the literature by Bircher et al. (2012), El Hajj et al. (2018) and Ma et al. (2019), as well as surface effects (i.e., surface roughness, land-cover heterogeneity within the pixel) usually smoothed when observing at larger scale.

As showed in Fig. 2 and Table 3 (and in their summary in Table 4), in terms of Pearson's correlation coefficient, it was highlighted the complementarity SMAP L4 and ESA CCI in agreement with those found by Ma et al. (2019) at the global scale. However, we found in line with Cui et al. (2017) that SMOS-IC had good and comparable correlation over the REMEDHUS network used to describe the 793 ecoregion and in Denmark within the 647 ecoregion.

In terms of ubRMSE, in line with the concept of complementarity, ESA CCI was superior to the SMAP L4. Consistent with Al-Yaari et al. (2019) who obtained lower performances of most remotely sensed SM products in "cold climate" areas (e.g., Koppen-Geiger D), we observed in Fig. 2 for ecoregion 679 an ubRMSE greater than 0.1 for all satellite products, as expected due to the effects of snow, frozen conditions and landscape. However, we should mention that the concurrence of disturbing factors, such as dense vegetation or mountains, could further alter the analysis performance in some of the ecoregions.

Concerning to bias, SMAP L4 and ESA CCI tend to overestimate the in situ ISMN SM, SMOS-IC and CGLS is prone to underestimate in situ SM. It is worth noting that the use, in our study, of Gleeson's porosity map to rescaled CGLS and ASCAT measurement units for a consistent comparison with other satellite products, as highlighted by Fascetti et al. (2016), can influence the results.

What particularly stands out from the r/r$_{ANOM}$ comparison, as showed in Table 3, was the confirmation of the best results in addition to other performance metrics for all the remote sensing products in the case of the Baltic mixed forests (647) or Balkan mixed forests (646) but also Iberian sclerophyllous and semi-deciduous forests (793).

On the other hand, all SM satellite products showed the high signal variability due to the screening of anomaly outliers (r$_{ANOM}$ greater than r) in the central European mixed forest ecoregion (654). Moreover, SMAP L4, which has proved to be the most accurate SM product in our

analysis, showed a similar effect in performance also for the Pontic steppe (735) ecoregion, as well as it has been shown in the case of ESA CCI. This indicates that Central European mixed forest ecoregion (654) and Pontic steppe (735) ecoregions are critical areas to obtain accurate SM assessment via the selected satellite products.

Focusing on all results metrics of SMAP L4, it achieved correlation around 0.7, the best values of ubRMSE and the highest performance in terms of r/r$_{ANOM}$ on the ecoregion group (cluster 1 in Fig. 3) constituted by 644, 646, 647 and 648. Similarly, the ecoregions of Mediterranean area (cluster 2 in Fig. 3: 793,795 and 799) showed all a quite high performance with r around 0.66, ubRMSE around 0.07 and r > r$_{ANOM}$. Meanwhile, as said above, on the group (cluster 3 in Fig. 3) of 654 and 735, SMAP L4 reached low performances. Due to similar performances and as geographically contiguous areas, 679 and 717 could be considered as another group (cluster 4 in Fig. 3). In the rest part of ecoregions, it demonstrated also significative performances (r > 0.5 and r > r$_{ANOM}$) but without a particular common pattern (cluster 5 in Fig. 3).

Hence, we used the ERA5-Land data, a reanalysis dataset providing at ~9 km grid spacing and covering the period from 1950 to 2–3 months before the present, to find similarity inside each cluster or dissimilarity from one cluster to other that can support performances' results. The core of ERA5-Land, i.e., a reproduction of the land component of the ERA5 climate reanalysis, forced by the ERA5 weather fields, is the Tiled ECMWF Scheme for Surface Exchanges over Land that incorporates land surface hydrology (H-TESSEL). It uses the CY45R1 version of the IFS (https://confluence.ecmwf.int/display/CKB/ERA5-Land%3A+data+documentation). In particular, we have downloaded the data for each month of the period 2015–2020 for air temperature (2m_temperature: temperature of air at 2 m above the surface of land, sea or in-land waters), precipitation (total_precipitation: sum of large-scale precipitation and convective precipitation), evaporation (total_evaporation: accumulated amount of water that has evaporated from the Earth's surface) and Leaf Area Index of high and low vegetation (leaf_area_index_high_vegetation, leaf_area_index_low_vegetation). Thus, we have computed for each variable the annual mean, maximum and minimum.

The first cluster of ecoregions (644–646–647–648), where SMAP L4 showed the highest performance for most part of the metrics, was characterized by heavy rain, intermediate vegetation level and
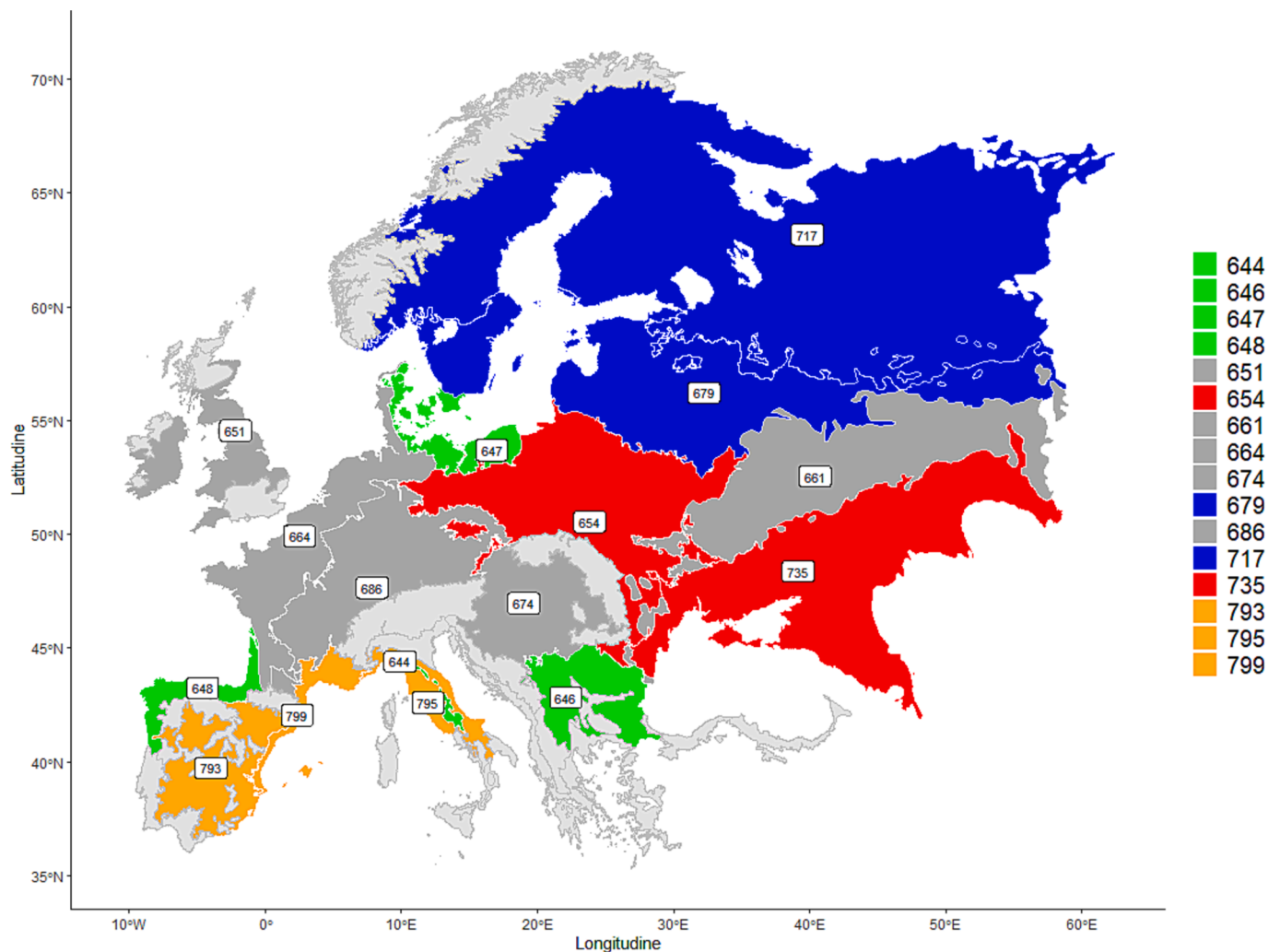
Fig. 3. Ecoregions grouped by clusters derived from performances (especially r using the top performer SMAP L4).

moderate evaporation (the air temperature did not give additional information). The ecoregions 793,795 and 799, were all in the Mediterranean and were characterized by low precipitation and evaporation and high temperature.

The remaining part of ecoregions presents a diversity of results in term of metrics without a common pattern in the ERA5-Land data. An exception is the cluster 4 (679–717), in which only SMAP L4 obtained fair good results and the ERA5-Land indicates the coldest climates among all ecoregions (3–6 degrees average) and lowest evaporation. In addition, in those areas, there are few stations to characterize large areas where soils are cold and sparsely vegetated.

The Central European mixed forest (654) and Pontic steppe (735) ecoregions (cluster 3) were areas in which we cannot obtain accurate SM assessment via the selected satellite products, and apparently, they seem to do not have any common characteristics in term of vegetation and climate. However, if we look at the comparison in term of SM using SMAP L4 satellite product with both in situ and ERA5-Land SM (volumetric_soil_water_layer_1: volume of water in soil layer 1 for a depth that goes from 0 to 7 cm), as showed in Fig. 4, we highlighted that SMAP L4 and ERA5-Land SM were good correlated in these ecoregions (graph in the middle). But similar to SMAP L4 vs ISMN correlation (on the left of Fig. 4), the ERA5-Land vs ISMN correlation (on the right of Fig. 4) was very low. This can suggest a possible inconsistency or a high uncertainty in the in-situ data. Moreover, there could be additional climatic and physical factors, e.g., subsurface scatterers, which may be the causes of uncorrelation. Wagner et al. (2022) recently demonstrated how in more

temperate climatic regions, strong subsurface scatterers (e.g., karstic rock) may become detectable during dry spells, especially when they are near the soil surface, adding uncertainty in the retrieved soil moisture value. Our results, indeed, indicate for sure problems in some areas that affected the continental scale analysis performed (please see last row of Table 3). In fact, the inclusion of these areas can affect the overall performance of SM products, hence producing the variegate results that several past studies have found in Europe.

It was nothing as for some of the ecoregions was more complicated to extract a clear picture of their behavior since an ecoregion is for its nature a combination of climate, soil, vegetation and results of remote sensing inter-comparison does not show a marked trend or a singular direction. However, our work provides useful insights about SM products performance not achievable when regional, continental or global scale are considered and should support future studies in ranking various SM products for various application in different location of Europe.

5. Conclusion

In the present work, we assessed an intercomparison between five SM satellite retrievals using the ISMN SM data as reference dataset, on European Ecoregions, homogeneous zone based on vegetation as climatic characteristics. Satellite SM products come from active (H115 & H116, CGLS SSM 1 km), passive (SMAP L4, SMOS-IC) or combined sensors (ESA CCI). Modelled (SMAP L4), blended (ESA CCI) and not
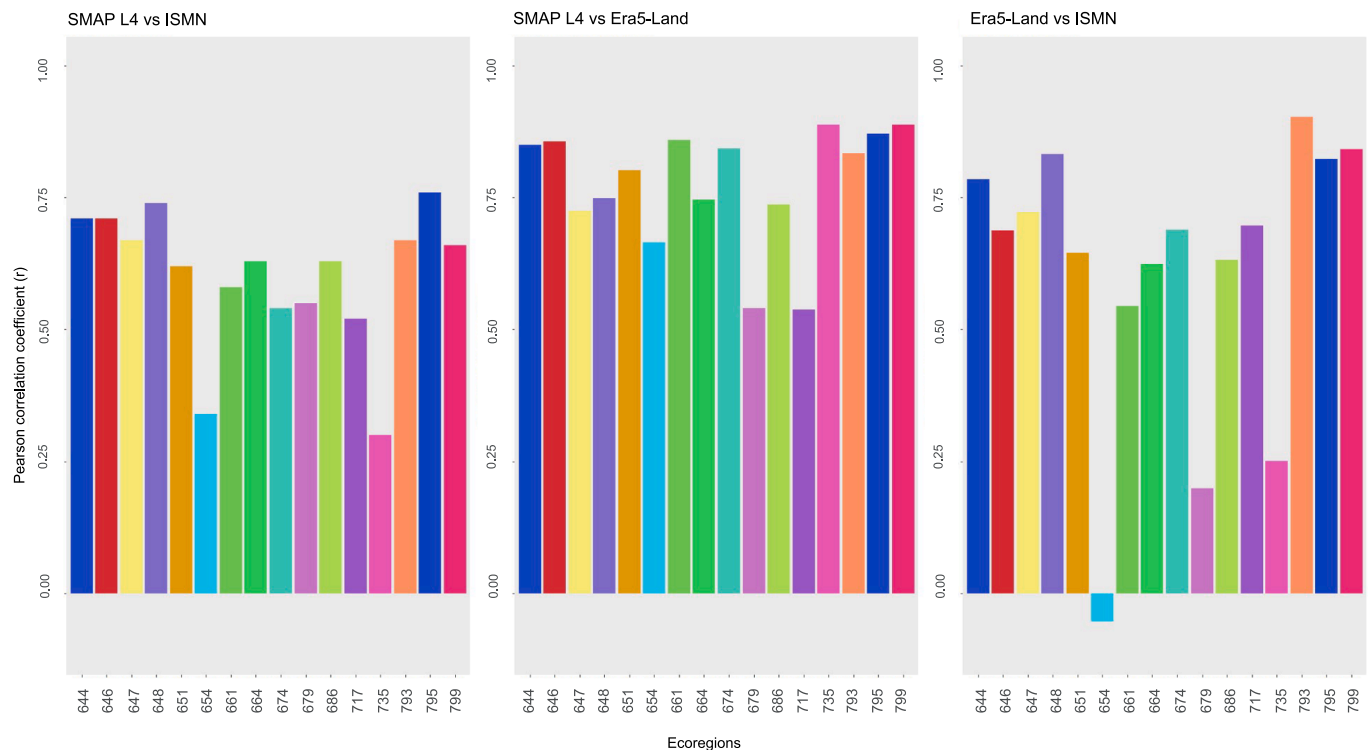
Fig. 4. Comparison of Pearson correlation coefficient across ecoregions on SM values between SMAP L4 and ISMN (on the left), SMAP L4 and ERA 5 LAND (in the middle), and ERA 5 LAND and ISMN (on the right).

modelled/blended data (SMOS – IC; ASCAT; CGLS 1 km) have been tested transforming all data in unit of volumetric water content (VWC) using a porosity map.

Results demonstrate that SMAP L4 shows the best performances regardless of the considered metrics, ESA CCI is the product ranking just below it and can be considered as complementary with SMAP L4, depending on the type of performance considered. ASCAT provided the best results among non-modelled/blended SM satellite products, achieving a meaningful correlation on seven ecoregions. For those ecoregions where ESA CCI has the highest level of accuracy, ASCAT shows good performance, highlighting its fundamental role in the blended ESA CCI product. CGLS SSM 1 km had the lowest performance and was the nosiest SM satellite retrieval exploited. The use of SM anomalies computed on a 35-day moving window gave results consistent the one already discussed, indicating SMAP L4 as the most accurate product.

There were a few ecoregions clusters characterized by common feature in terms of climate or vegetations such as the areas where all these products are most reliable (made by ecoregions as the Cantabrian Mixed forests or the Balkan Mixed forests) or high performing regardless satellite, e.g., ecoregions which belong to Mediterranean area. In addition, the comparison, in terms of SM, between SMAP L4, ISMN with ERA5-Land allowed us to justify the worst performances of all the satellite products in the Central European Mixed forests (654) and the Pontic steppe (735) showing a poor correlation between ISMN and ERA5-Land and a good correlation between SMAP L4 and ERA5-Land that could indicative of some issues in the ground-based network whose stations are shared between 654 and 735. Nevertheless, our work provided information about the assessment of SM satellite retrievals which could be lost if analysis at regional, continental or global scale are considered and should support future studies on Europe. For example, the future work could deeper investigate the lack of correlation between all SM satellites and ISMN shallow SM ground measurements removing completely the seasonality or by analyzing the phenological cycle, with the aim to led to a more complete characterization of the hydrological

features of the ecoregions.

Declaration of Competing Interest

The authors declare that they have no known competing financial interests or personal relationships that could have appeared to influence the work reported in this paper.

Data availability

Data will be made available on request.

Appendix A. Supplementary data

Supplementary data to this article can be found online at https://doi.org/10.1016/j.jhydrol.2023.130311.

References

Al-Yaari, A., Wigneron, J.-P., Ducharne, A., Kerr, Y., De Rosnay, P., De Jeu, R., Govind, A., Al Bitar, A., Albergel, C., Munoz-Sabater, J., et al., 2014. Global-scale evaluation of two satellite-based passive microwave soil moisture datasets (SMOS and AMSR-E) with respect to Land Data Assimilation System estimates. Remote Sens. Environ. 149, 181–195.

Al-Yaari, A., Wigneron, J.-P., Dorigo, W., Colliander, A., Pellarin, T., Hahn, S., Mialon, A., Richaume, P., Fernandez-Moran, R., Fan, L., Kerr, Y.H., De Lannoy, G., 2019. Assessment and inter-comparison of recently developed/reprocessed microwave satellite soil moisture products using ISMN ground-based measurements. Remote Sens. Environ. 224, 289–303. https://doi.org/10.1016/j.rse.2019.02.008.

Albano, R., Manfreda, S., Celano, G., 2017. MY SIRR: Minimalist agro-hYdrological model for Sustainable IRRigation management—Soil moisture and crop dynamics. SoftwareX 6, 107–117. https://doi.org/10.1016/j.softx.2017.04.005.

Baldwin, D., Manfreda, S., Keller, K., Smithwick, E.A.H., 2017. Predicting root zone soil moisture with soil properties and satellite near-surface moisture data across the

conterminous United States. J. Hydrol. 546, 393–404. https://doi.org/10.1016/j.jhydrol.2017.01.020.

Baldwin, D., Manfreda, S., Lin, H., Smithwick, E.A.H., 2019. Estimating root zone soil moisture across the eastern united states with passive microwave satellite data and a simple hydrologic model. Remote Sens. (Basel) 11, 2013. https://doi.org/10.3390/rs11172013.

Bauer-Marschallinger, B., Freeman, V., Cao, S., Paulik, C., Schaufler, S., Stachl, T., Modanesi, S., Massari, C., Ciabatta, L., Brocca, L., Wagner, W., 2019. Toward global soil moisture monitoring with sentinel-1: harnessing assets and overcoming obstacles. IEEE Trans. Geosci. Remote Sensing 57, 520–539. https://doi.org/10.1109/TGRS.2018.2858004.

Bircher, S., Skou, N., Jensen, K.H., Walker, J.P., Rasmussen, L., 2012. A soil moisture and temperature network for SMOS validation in Western Denmark. Hydrol. Earth Syst. Sci. 16, 1445–1463.

Brocca, L., Melone, F., Moramarco, T., Morbidelli, R., 2009. Soil moisture temporal stability over experimental areas in Central Italy. Geoderma 148, 364–374. https://doi.org/10.1016/j.geoderma.2008.11.004.

Brocca, L., Hasenauer, S., Lacava, T., Melone, F., Moramarco, T., Wagner, W., Dorigo, W., Matgen, P., Martínez-Fernández, J., Llorens, P., et al., 2011. Soil moisture estimation through ASCAT and AMSR-E sensors: An intercomparison and validation study across Europe. Remote Sens. Environ. 115, 3390–3408.

Bulgarini, F., Teofili, C., Bologna, G., 2004. Global 200 ERC, Ecoregional Conservation. Il processo di conservazione.

Chen, F., Crow, W.T., Colliander, A., Cosh, M.H., Jackson, T.J., Bindlish, R., Reichle, R. H., Chan, S.K., Bosch, D.D., Starks, P.J., Goodrich, D.C., Seyfried, M.S., 2017. Application of triple collocation in ground-based validation of soil moisture active/passive (SMAP) Level 2 data products. IEEE J Sel. Top. Appl. Earth Observations Remote Sensing 10, 489–502. https://doi.org/10.1109/JSTARS.2016.2569998.

Colliander, A., Jackson, T.J., Bindlish, R., Chan, S., Das, N., Kim, S.B., Cosh, M.H., Dunbar, R.S., Dang, L., Pashaian, L., Asanuma, J., Aida, K., Berg, A., Rowlandson, T., Bosch, D., Caldwell, T., Caylor, K., Goodrich, D., al Jassar, H., Lopez-Baeza, E., Martínez-Fernández, J., González-Zamora, A., Livingston, S., McNairn, H., Pacheco, A., Moghaddam, M., Montzka, C., Notarnicola, C., Niedrist, G., Pellarin, T., Prueger, J., Pulliainen, J., Rautiainen, K., Ramos, J., Seyfried, M., Starks, P., Su, Z., Zeng, Y., van der Velde, R., Thibeault, M., Dorigo, W., Vreugdenhil, M., Walker, J.P., Wu, X., Monerris, A., O'Neill, P.E., Entekhabi, D., Njoku, E.G., Yueh, S., 2017. Validation of SMAP surface soil moisture products with core validation sites. Remote Sens. Environ. 191, 215–231. https://doi.org/10.1016/j.rse.2017.01.021.

Cosh, M.H., Jackson, T.J., Starks, P., Heathman, G., 2006. Temporal stability of surface soil moisture in the Little Washita River watershed and its applications in satellite soil moisture product validation. J. Hydrol. 323, 168–177. https://doi.org/10.1016/j.jhydrol.2005.08.020.

Cui, C., Xu, J., Zeng, J., Chen, K.-S., Bai, X., Lu, H., Chen, Q., Zhao, T., 2017. Soil moisture mapping from satellites: An intercomparison of SMAP, SMOS, FY3B, AMSR2, and ESA CCI over two dense network regions at different spatial scales. Remote Sens. (Basel) 10, 33.

Dasmann, R. F., 1973. A system for defining and classifying natural regions for purposes of conservation. Morges (Switzerland): International Union for Conservation of Nature and Natural Resources. IUCN Occasional Paper no. 7.

Dasmann, R. F., 1974. Biotic provinces of the world: Further development of a system for defining and classifying natural regions for purposes of conservation. Morges (Switzerland): International Union for Conservation of Nature and Natural Resources. IUCN Occasional Paper no. 9.

Derksen, C., Xu, X., Scott Dunbar, R., Colliander, A., Kim, Y., Kimball, J.S., Black, T.A., Euskirchen, E., Langlois, A., Loranty, M.M., Marsh, P., Rautiainen, K., Roy, A., Royer, A., Stephens, J., 2017. Retrieving landscape freeze/thaw state from Soil Moisture Active Passive (SMAP) radar and radiometer measurements. Remote Sens. Environ. 194, 48–62. https://doi.org/10.1016/j.rse.2017.03.007.

Dinerstein, E., Olson, D., Joshi, A., Vynne, C., Burgess, N.D., Wikramanayake, E., Hahn, N., Palminteri, S., Hedao, P., Noss, R., et al., 2017. An ecoregion-based approach to protecting half the terrestrial realm. Bioscience 67, 534–545.

Dorigo, W., Oevelen, P., Wagner, W., Drusch, M., Mecklenburg, S., Robock, A., Jackson, T., 2011. A new international network for in situ soil moisture data. Eos Trans. AGU 92, 141–142. https://doi.org/10.1029/2011EO170001.

Dorigo, W.A., Xaver, A., Vreugdenhil, M., Gruber, A., Hegyiová, A., Sanchis-Dufau, A.D., Zamojski, D., Cordes, C., Wagner, W., Drusch, M., 2013. Global automated quality control of in situ soil moisture data from the international soil moisture network. Vadose Zone J. 12 (vzj2012), 0097. https://doi.org/10.2136/vzj2012.0097.

Dorigo, W., Wagner, W., Albergel, C., Albrecht, F., Balsamo, G., Brocca, L., Chung, D., Ertl, M., Forkel, M., Gruber, A., Haas, E., Hamer, P.D., Hirschi, M., Ikonen, J., de Jeu, R., Kidd, R., Lahoz, W., Liu, Y.Y., Miralles, D., Mistelbauer, T., Nicolai-Shaw, N., Parinussa, R., Pratola, C., Reimer, C., van der Schalie, R., Seneviratne, S.I., Smolander, T., Lecomte, P., 2017. ESA CCI Soil Moisture for improved Earth system understanding: State-of-the art and future directions. Remote Sens. Environ. 203, 185–215. https://doi.org/10.1016/j.rse.2017.07.001.

Dorigo, W., Himmelbauer, I., Aberer, D., Schremmer, L., Petrakovic, I., Zappa, L., Preimesberger, W., Xaver, A., Annor, F., Ardö, J., Baldocchi, D., Bitelli, M., Blöschl, G., Bogena, H., Brocca, L., Calvet, J.-C., Camarero, J.J., Capello, G., Choi, M., Cosh, M.C., van de Giesen, N., Hajdu, I., Ikonen, J., Jensen, K.H., Kanniah, K.D., de Kat, I., Kirchengast, G., Kumar Rai, P., Kyrouac, J., Larson, K., Liu, S., Loew, A., Moghaddam, M., Martínez Fernández, J., Mattar Bader, C., Morbidelli, R., Musial, J.P., Osenga, E., Palecki, M.A., Pellarin, T., Petropoulos, G.P., Pfeil, I., Powers, J., Robock, A., Rüdiger, C., Rummel, U., Strobel, M., Su, Z., Sullivan, R., Tagesson, T., Varlagin, A., Vreugdenhil, M., Walker, J., Wen, J., Wenger, F., Wigneron, J.P., Woods, M., Yang, K., Zeng, Y., Zhang, X., Zreda, M., Dietrich, S., Gruber, A., van Oevelen, P., Wagner, W., Scipal, K., Drusch, M.,

Sabia, R., 2021. The International Soil Moisture Network: serving Earth system science for over a decade. Hydrol. Earth Syst. Sci. 25, 5749–5804. https://doi.org/10.5194/hess-25-5749-2021.

El Hajj, M., Baghdadi, N., Zribi, M., Rodríguez-Fernández, N., Wigneron, J.P., Al-Yaari, A., Al Bitar, A., Albergel, C., Calvet, J.-C., 2018. Evaluation of SMOS, SMAP, ASCAT and Sentinel-1 soil moisture products at sites in Southwestern France. Remote Sens. (Basel) 10, 569.

Entekhabi, D., Njoku, E.G., O'Neill, P.E., Kellogg, K.H., Crow, W.T., Edelstein, W.N., Entin, J.K., Goodman, S.D., Jackson, T.J., Johnson, J., Kimball, J., Piepmeier, J.R., Koster, R.D., Martin, N., McDonald, K.C., Moghaddam, M., Moran, S., Reichle, R., Shi, J.C., Spencer, M.W., Thurman, S.W., Tsang, L., Van Zyl, J., 2010a. The Soil Moisture Active Passive (SMAP) Mission. Proc. IEEE 98, 704–716. https://doi.org/10.1109/JPROC.2010.2043918.

Entekhabi, D., Reichle, R.H., Koster, R.D., Crow, W.T., 2010b. Performance metrics for soil moisture retrievals and application requirements. J. Hydrometeorol. 11, 832–840. https://doi.org/10.1175/2010JHM1223.1.

Escorihuela, M.-J., Chanzy, A., Wigneron, J.-P., Kerr, Y.H., 2010. Effective soil moisture sampling depth of L-band radiometry: A case study. Remote Sens. Environ. 114, 995–1001.

Fascetti, F., Pierdicca, N., Pulvirenti, L., Crapolicchio, R., Muñoz-Sabater, J., 2016. A comparison of ASCAT and SMOS soil moisture retrievals over Europe and Northern Africa from 2010 to 2013. Int. J. Appl. Earth Obs. Geoinf. 45, 135–142.

Fernandez-Moran, R., Al-Yaari, A., Mialon, A., Mahmoodi, A., De Lannoy, G., Rodriguez-Fernandez, N., Lopez-Baeza, E., Kerr, Y., Wigneron, J.-P., 2017. SMOS-IC: an alternative SMOS soil moisture and vegetation optical depth product. Remote Sens. (Basel) 9, 457. https://doi.org/10.3390/rs9050457.

Friedl, M.A., Strahler, A.H., Hodges, J., 2010. ISLSCP II MODIS (Collection 4) IGBP Land Cover, 2000-2001 3.564251 MB. 10.3334/ORNLDAAC/968.

Gao, H., Wood, E.F., Jackson, T.J., Drusch, M., Bindlish, R., 2006. Using TRMM/TMI to retrieve surface soil moisture over the Southern United States from 1998 to 2002. J. Hydrometeorol. 7, 23–38. https://doi.org/10.1175/JHM473.1.

Gleeson, T., Moosdorf, N., Hartmann, J., van Beek, L.P.H., 2014. A glimpse beneath earth's surface: GLobal HYdrogeology MaPS (GLHYMPS) of permeability and porosity. Geophys. Res. Lett. 41, 3891–3898. https://doi.org/10.1002/2014GL059856.

Gruber, A., Scanlon, T., van der Schalie, R., Wagner, W., Dorigo, W., 2019. Evolution of the ESA CCI Soil Moisture climate data records and their underlying merging methodology. Earth Syst. Sci. Data 11, 717–739. https://doi.org/10.5194/essd-11-717-2019.

Kerr, Y.H., Waldteufel, P., Wigneron, J.-P., Delwart, S., Cabot, F., Boutin, J., Escorihuela, M.-J., Font, J., Reul, N., Gruhier, C., Juglea, S.E., Drinkwater, M.R., Hahne, A., Martín-Neira, M., Mecklenburg, S., 2010. The SMOS mission: new tool for monitoring key elements of the global water cycle. Proc. IEEE 98, 666–687. https://doi.org/10.1109/JPROC.2010.2043032.

Kerr, Y.H., 2007. Soil moisture from space: Where are we? Hydrgeol. J. 15, 117–120. https://doi.org/10.1007/s10040-006-0095-3.

Koster, R.D., Dirmeyer, P.A., Guo, Z., Bonan, G., Chan, E., Cox, P., Gordon, C.T., Kanae, S., Kowalczyk, E., Lawrence, D., Liu, P., Lu, C.-H., Malyshev, S., McAvaney, B., Mitchell, K., Mocko, D., Oki, T., Oleson, K., Pitman, A., Sud, Y.C., Taylor, C.M., Verseghy, D., Vasic, R., Xue, Y., Yamada, T., 2004. Regions of strong coupling between soil moisture and precipitation. Science 305, 1138–1140. https://doi.org/10.1126/science.1100217.

Lacava, T., Matgen, P., Brocca, L., Bittelli, M., Pergola, N., Moramarco, T., Tramutoli, V., 2012. A first assessment of the SMOS soil moisture product with in situ and modeled data in Italy and Luxembourg. IEEE Trans. Geosci. Remote Sens. 50, 1612–1622.

Lacava, T., Coviello, I., Faruolo, M., Mazzeo, G., Pergola, N., Tramutoli, V., 2013. A multitemporal investigation of AMSR-E C-band radio-frequency interference. IEEE Trans. Geosci. Remote Sensing 51, 2007–2015. https://doi.org/10.1109/TGRS.2012.2228487.

Li, X., Al-Yaari, A., Schwank, M., Fan, L., Frappart, F., Swenson, J., Wigneron, J.-P., 2020. Compared performances of SMOS-IC soil moisture and vegetation optical depth retrievals based on Tau-Omega and Two-Stream microwave emission models. Remote Sens. Environ. 236, 111502.

Li, X., Wigneron, J.-P., Frappart, F., Fan, L., Ciais, P., Fensholt, R., Entekhabi, D., Brandt, M., Konings, A.G., Liu, X., et al., 2021. Global-scale assessment and inter-comparison of recently developed/reprocessed microwave satellite vegetation optical depth products. Remote Sens. Environ. 253, 112208.

Liu, Y.Y., Parinussa, R.M., Dorigo, W.A., De Jeu, R.A.M., Wagner, W., Van Dijk, A.I.J.M., McCabe, M.F., Evans, J.P., 2011. Developing an improved soil moisture dataset by blending passive and active microwave satellite-based retrievals. Hydrol. Earth Syst. Sci. 15, 425–436. https://doi.org/10.5194/hess-15-425-2011.

Liu, Y., Liu, Y., Wang, W., 2019. Inter-comparison of satellite-retrieved and global land data assimilation system-simulated soil moisture datasets for global drought analysis. Remote Sens. Environ. 220, 1–18. https://doi.org/10.1016/j.rse.2018.10.026.

Loew, A., Schlenz, F., 2011. A dynamic approach for evaluating coarse scale satellite soil moisture products. Hydrol. Earth Syst. Sci. 15, 75–90. https://doi.org/10.5194/hess-15-75-2011.

Ma, H., Zeng, J., Chen, N., Zhang, X., Cosh, M.H., Wang, W., 2019. Satellite surface soil moisture from SMAP, SMOS, AMSR2 and ESA CCI: A comprehensive assessment using global ground-based observations. Remote Sens. Environ. 231, 111215 https://doi.org/10.1016/j.rse.2019.111215.

Manfreda, S., Lacava, T., Onorati, B., Pergola, N., Di Leo, M., Margiotta, M.R., Tramutoli, V., 2011. On the use of AMSU-based products for the description of soil water content at basin scale. Hydrol. Earth Syst. Sci. 15, 2839–2852. https://doi.org/10.5194/hess-15-2839-2011.

Manfreda, S., Brocca, L., Moramarco, T., Melone, F., Sheffield, J., 2014. A physically based approach for the estimation of root-zone soil moisture from surface measurements. Hydrol. Earth Syst. Sci. 18, 1199–1212.

Min, X., Shangguan, Y., Huang, J., Wang, H., Shi, Z., 2022. Relative strengths recognition of nine mainstream satellite-based soil moisture products at the global scale. Remote Sens. (Basel) 14, 2739. https://doi.org/10.3390/rs14122739.

Miralles, D.G., van den Berg, M.J., Teuling, A.J., de Jeu, R.A.M., 2012. Soil moisture-temperature coupling: A multiscale observational analysis: soil moisture-temperature coupling. Geophys. Res. Lett. 39, n/a-n/a. https://doi.org/10.1029/2012GL053703.

Mohammed, P.N., Aksoy, M., Piepmeier, J.R., Johnson, J.T., Bringer, A., 2016. SMAP L-band microwave radiometer: RFI mitigation prelaunch analysis and first year on-orbit observations. IEEE Trans. Geosci. Remote Sensing 54, 6035–6047. https://doi.org/10.1109/TGRS.2016.2580459.

Ochsner, T.E., Cosh, M.H., Cuenca, R.H., Dorigo, W.A., Draper, C.S., Hagimoto, Y., Kerr, Y.H., Larson, K.M., Njoku, E.G., Small, E.E., et al., 2013. State of the art in large-scale soil moisture monitoring. Soil Sci. Soc. Am. J. 77, 1888–1919.

Oliva, R., Daganzo, E., Kerr, Y.H., Mecklenburg, S., Nieto, S., Richaume, P., Gruhier, C., 2012. SMOS radio frequency interference scenario: Status and actions taken to improve the RFI environment in the 1400–1427-MHz passive band. IEEE Trans. Geosci. Remote Sens. 50, 1427–1439.

Olson, D.M., Dinerstein, E., 1998. The Global 200: A representation approach to conserving the Earth's most biologically valuable ecoregions. Conserv. Biol. 12, 502–515. https://doi.org/10.1046/j.1523-1739.1998.012003502.x.

Olson, D.M., Dinerstein, E., 2002. The Global 200: priority ecoregions for global conservation. Ann. Mo. Bot. Gard. 199–224.

Olson, D.M., Dinerstein, E., Wikramanayake, E.D., Burgess, N.D., Powell, G.V.N., Underwood, E.C., D'amico, J.A., Itoua, I., Strand, H.E., Morrison, J.C., Loucks, C.J., Allnutt, T.F., Ricketts, T.H., Kura, Y., Lamoreux, J.F., Wettengel, W.W., Hedao, P., Kassem, K.R., 2001. Terrestrial Ecoregions of the World: A new map of life on Earth. Bioscience 51, 933. https://doi.org/10.1641/0006-3568(2001)051[0933:TEOTWA]2.0.CO;2.

Parrens, M., Wigneron, J.-P., Richaume, P., Mialon, A., Al Bitar, A., Fernandez-Moran, R., Al-Yaari, A., Kerr, Y.H., 2016. Global-scale surface roughness effects at L-band as estimated from SMOS observations. Remote Sens. Environ. 181, 122–136. https://doi.org/10.1016/j.rse.2016.04.006.

Pathe, C., Wagner, W., Sabel, D., Doubkova, M., Basara, J.B., 2009. Using ENVISAT ASAR global mode data for surface soil moisture retrieval over Oklahoma, USA. IEEE Trans. Geosci. Remote Sens. 47, 468–480.

Peng, J., Tanguy, M., Robinson, E.L., Pinnington, E., Evans, J., Ellis, R., Cooper, E., Hannaford, J., Blyth, E., Dadson, S., 2021. Estimation and evaluation of high-resolution soil moisture from merged model and Earth observation data in the Great Britain. Remote Sens. Environ. 264, 112610 https://doi.org/10.1016/j.rse.2021.112610.

Porporato, A., Rodriguez-Iturbe, I., 2002. Ecohydrology-a challenging multidisciplinary research perspective / Ecohydrologie: une perspective stimulante de recherche multidisciplinaire. Hydrol. Sci. J. 47, 811–821. https://doi.org/10.1080/02626660209492985.

Qiu, J., Crow, W.T., Nearing, G.S., 2016. The impact of vertical measurement depth on the information content of soil moisture for latent heat flux estimation. J. Hydrometeorol. 17, 2419–2430. https://doi.org/10.1175/JHM-D-16-0044.1.

Ray, R., Fares, A., He, Y., Temimi, M., 2017. Evaluation and inter-comparison of satellite soil moisture products using in situ observations over Texas, U.S. Water 9, 372. https://doi.org/10.3390/w9060372.

Reichle, R.H., De Lannoy, G.J., Forman, B.A., Draper, C.S., Liu, Q., 2014. Connecting satellite observations with water cycle variables through land data assimilation: Examples using the NASA GEOS-5 LDAS. Surv. Geophys. 35, 577–606.

Ricketts, T.H., Dinerstein, E., Olson, D.M., Eichbaum, W., Loucks, C.J., DellaSala, D.A., Kavanagh, K., Hedao, P., Hurley, P., Carney, K., et al., 1999. Terrestrial Ecoregions of North America: A Conservation Assessment. Island Press.

Rodell, M., Houser, P., Jambor, U., Gottschalck, J., Mitchell, K., Meng, C.-J., Arsenault, K., Cosgrove, B., Radakovich, J., Bosilovich, M., et al., 2004. The global land data assimilation system. Bull. Am. Meteorol. Soc. 85, 381–394.

Rodríguez-Fernández, N., Kerr, Y., van der Schalie, R., Al-Yaari, A., Wigneron, J.-P., de Jeu, R., Richaume, P., Dutra, E., Mialon, A., Drusch, M., 2016. Long Term Global Surface Soil Moisture Fields Using an SMOS-Trained Neural Network Applied to AMSR-E Data. Remote Sensing 8, 959. https://doi.org/10.3390/rs8110959.

Rodríguez-Fernández, N.J., Muñoz Sabater, J., Richaume, P., de Rosnay, P., Kerr, Y.H., Albergel, C., Drusch, M., Mecklenburg, S., 2017. SMOS near-real-time soil moisture product: processor overview and first validation results. Hydrol. Earth Syst. Sci. 21, 5201–5216. https://doi.org/10.5194/hess-21-5201-2017.

Rodríguez-Iturbe, I., Isham, V., Cox, D.R., Manfreda, S., Porporato, A., 2006. Space-time modeling of soil moisture: Stochastic rainfall forcing with heterogeneous vegetation: space-time modeling of soil moisture. Water Resour. Res. 42 https://doi.org/10.1029/2005WR004497.

Rubel, F., Brugger, K., Haslinger, K., Auer, I., 2017. The climate of the European Alps: Shift of very high resolution Köppen-Geiger climate zones 1800–2100. Meteorol. Z. 26, 115–125.

Rübel, E.,1930. Pflanzengesellschaften der Erde. Berlin: Hans Huber.

Scarpino, S., Albano, R., Cantisani, A., Mancusi, L., Sole, A., Milillo, G., 2018. Multitemporal SAR data and 2D hydrodynamic model flood scenario dynamics assessment. ISPRS Int. J. Geo Inf. 7, 105.

Scipal, K., Holmes, T., De Jeu, R., Naeimi, V., Wagner, W., 2008. A possible solution for the problem of estimating the error structure of global soil moisture data sets. Geophys. Res. Lett. 35.

Seneviratne, S.I., Corti, T., Davin, E.L., Hirschi, M., Jaeger, E.B., Lehner, I., Orlowsky, B., Teuling, A.J., 2010. Investigating soil moisture–climate interactions in a changing climate: A review. Earth Sci. Rev. 99, 125–161. https://doi.org/10.1016/j.earscirev.2010.02.004.

Starks, P.J., Heathman, G.C., Jackson, T.J., Cosh, M.H., 2006. Temporal stability of soil moisture profile. J. Hydrol. 324, 400–411.

Tavakol, A., Rahmani, V., Quiring, S.M., Kumar, S.V., 2019. Evaluation analysis of NASA SMAP L3 and L4 and SPoRT-LIS soil moisture data in the United States. Remote Sens. Environ. 229, 234–246. https://doi.org/10.1016/j.rse.2019.05.006.

[UNESCO] United Nations Educational, Scientific and Cultural Organization 1969. A Framework for a Classification of World Vegetation. Paris: UNESCO. UNESCO SC//WS//269.

Vachaud, G., Passerat De Silans, A., Balabanis, P., Vauclin, M., 1985. Temporal stability of spatially measured soil water probability density function. Soil Sci. Soc. Am. J. 49, 822–828. https://doi.org/10.2136/sssaj1985.03615995004900040006x.

Wagner, W., Lemoine, G., Rott, H., 1999. A method for estimating soil moisture from ERS scatterometer and soil data. Remote Sens. Environ. 70, 191–207. https://doi.org/10.1016/S0034-4257(99)00036-X.

Wagner, W., Blöschl, G., Pampaloni, P., Calvet, J.-C., Bizzarri, B., Wigneron, J.-P., Kerr, Y., 2007. Operational readiness of microwave remote sensing of soil moisture for hydrologic applications. Hydrol. Res. 38, 1–20. https://doi.org/10.2166/nh.2007.029.

Wagner, W., Hahn, S., Kidd, R., Melzer, T., Bartalis, Z., Hasenauer, S., Figa, J., De Rosnay, P., Jann, A., Schneider, S., et al., 2013. The ASCAT soil moisture product: A review of its. Meteorol. Z. 22, 1–29.

Wagner, W., Lindorfer, R., Melzer, T., Hahn, S., Bauer-Marschallinger, B., Morrison, K., Calvet, J.-C., Hobbs, S., Quast, R., Greimeister-Pfeil, I., et al., 2022. Widespread occurrence of anomalous C-band backscatter signals in arid environments caused by subsurface scattering. Remote Sens. Environ. 276, 113025.

Wagner, W., 1998. Soil moisture retrieval from ERS scatterometer data. Citeseer.

Walfish, S., 2006. A review of statistical outlier methods. Pharm. Technol. 30, 82.

Wigneron, J.-P., Kerr, Y., Waldteufel, P., Saleh, K., Escorihuela, M.-J., Richaume, P., Ferrazzoli, P., de Rosnay, P., Gurney, R., Calvet, J.-C., Grant, J.P., Guglielmetti, M., Hornbuckle, B., Mätzler, C., Pellarin, T., Schwank, M., 2007. L-band Microwave Emission of the Biosphere (L-MEB) Model: Description and calibration against experimental data sets over crop fields. Remote Sens. Environ. 107, 639–655. https://doi.org/10.1016/j.rse.2006.10.014.

Wigneron, J.-P., Fan, L., Ciais, P., Bastos, A., Brandt, M., Chave, J., Saatchi, S., Baccini, A., Fensholt, R., 2020. Tropical forests did not recover from the strong 2015–2016 El Niño event. Sci. Adv. 6, eaay4603. https://doi.org/10.1126/sciadv.aay4603.

Wigneron, J.-P., Li, X., Frappart, F., Fan, L., Al-Yaari, A., De Lannoy, G., Liu, X., Wang, M., Le Masson, E., Moisy, C., 2021. SMOS-IC data record of soil moisture and L-VOD: Historical development, applications and perspectives. Remote Sens. Environ. 254, 112238.

Zheng, J., Zhao, T., Lü, H., Shi, J., Cosh, M.H., Ji, D., Jiang, L., Cui, Q., Lu, H., Yang, K., Wigneron, J.-P., Li, X., Zhu, Y., Hu, L., Peng, Z., Zeng, Y., Wang, X., Kang, C.S., 2022. Assessment of 24 soil moisture datasets using a new in situ network in the Shandian River Basin of China. Remote Sens. Environ. 271, 112891 https://doi.org/10.1016/j.rse.2022.112891.